The EMBO Journal vol.15 no.14 pp.3579–3589, 1996

Structure of a specific peptide complex of the carboxy-terminal SH2 domain from the p85α subunit of phosphatidylinositol 3-kinase

Alexander L.Breeze[1], Bo V.Kara[2], Derek G.Barratt[2], Malcolm Anderson[2], John C.Smith[2], Richard W.Luke[3], J.Rick Best[3] and Susan A.Cartlidge[3]

Protein Structure Laboratory, [2]Biotechnology Department and [3]Cancer Research Department, Zeneca Pharmaceuticals, Mereside, Alderley Park, Cheshire SK10 4TG, UK

[1]Corresponding author

We have determined the solution structure of the C-terminal SH2 domain of the p85α subunit of human phosphatidylinositol (PI) 3-kinase (EC 2.7.1.137) in complex with a phosphorylated tyrosine pentapeptide sequence from the platelet-derived growth factor receptor using heteronuclear nuclear magnetic resonance spectroscopy. Overall, the structure is similar to other SH2 domain complexes, but displays different detail interactions within the phosphotyrosine binding site and in the recognition site for the +3 methionine residue of the peptide, the side chain of which inserts into a particularly deep and narrow pocket which is displaced relative to that of other SH2 domains. The contacts made within this +3 pocket provide the structural basis for the strong selection for methionine at this position which characterizes the SH2 domains of PI 3-kinase. Comparison with spectral and structural features of the uncomplexed domain shows that the long BG loop becomes less mobile in the presence of the bound peptide. In contrast, extreme resonance broadening encountered for most residues in the βD′, βE and βF strands and associated connecting loops of the domain in the absence of peptide persists in the complex, implying conformational averaging in this part of the molecule on a microsecond-to-millisecond time scale.

Keywords: NMR structure/phosphatidylinositol 3-kinase/phosphotyrosine peptide complex/SH2 domain/signal transduction

Introduction

Among the many mediators of the intracellular signalling processes that are switched on in response to extracellular stimuli is the lipid kinase phosphatidylinositol (PI) 3-kinase (reviewed by Kapeller and Cantley, 1994). Elaboration of 3-phosphorylated phosphoinositides, such as PI-3,4,5-tris-phosphate, by the 110 kDa catalytic subunit of this enzyme (p110; Hiles *et al.*, 1992) is a key mitogenic signal invoked by a wide variety of growth factors. The recruitment of PI 3-kinase to the substrate-rich plasma membrane locale occurs through recognition of specific tyrosine-phosphorylated, situated sequences on the cytoplasmic domains of activated growth factor receptor tyrosine kinases, by the enzyme's two Src-homology 2 (SH2) domains. These are contained within the 85 kDa regulatory subunit, p85 (Otsu *et al.*, 1991). The SH2 domain is a modular region of ~100 residues which occurs widely within intracellular signalling proteins (reviewed by Pawson and Schlessinger, 1993). Target specificity is conferred by the ability of different SH2 domains to bind preferentially to phosphotyrosine (pTyr) residues within certain sequence contexts. Studies using phosphopeptide libraries to probe sequence specificity have shown that, for example, the so-called group 1 SH2 domains of the non-receptor tyrosine kinases Src, Lck, Fyn and Abl, among others, display a preference for the motif pTyr–hydrophilic–hydrophilic–Ile/Pro (Songyang *et al.*, 1993). Another class of SH2 domain, including those of phospholipase C-γ1 (PLC-γ1), Syp tyrosine phosphatase and PI 3-kinase p85α itself, selects the general motif pTyr–hydrophobic–X–hydrophobic. Within this group (group 3; Songyang *et al.*, 1993), the p85α SH2 domains are notable for displaying a strong preference for methionine over all other amino acids at the +3 position following the pTyr; this preference is particularly marked in the case of the C-terminal domain (Songyang *et al.*, 1993). Known target sites for PI 3-kinase association with activated growth factor receptors include the sequences surrounding Tyr740 and Tyr751 of the kinase insert region of β-platelet-derived growth factor (PDGF) receptor, which become autophosphorylated upon binding of ligand (Kashishian *et al.*, 1992). Synthetic phosphotyrosine-containing peptides encompassing these sites bind with high affinity to recombinant p85α protein or to the individual expressed SH2 domains (Panayotou *et al.*, 1993; Piccione *et al.*, 1993), and are able to block PI 3-kinase association with the activated PDGF receptor (Escobedo *et al.*, 1991; Fantl *et al.*, 1992). Both SH2 domains have rather similar sequence specificity, binding the sequence contexts of either pTyr740 (pYMDM) or pTyr751 (pYVPM) with comparable affinity (Piccione *et al.*, 1993), although the C-terminal domain displays somewhat higher affinity (~10-fold) than the N-terminal domain (Klippel *et al.*, 1992; Panayotou *et al.*, 1993; Ponzetto *et al.*, 1993), and is slightly more promiscuous at the pY+1 position (Songyang *et al.*, 1993).

The structural features of SH2 domains and, in a number cases, of the interactions with their target peptide sequences have been elucidated by three-dimensional structures of free and peptide-complexed SH2 domains, determined both by X-ray crystallography and by nuclear magnetic resonance (NMR) spectroscopy. These include the unliganded N-terminal p85α (Booker *et al.*, 1992), Abl (Overduin *et al.*, 1992), Src (Waksman *et al.*, 1993) and N-terminal Syp (Lee *et al.*, 1994) SH2 domains; peptide–SH2 complexes of Src (Waksman *et al.*, 1992, 1993; Xu

et al., 1995), Lck (Eck *et al.*, 1993) and C-terminal PLC-γ1 (Pascal *et al.*, 1994a); and, more recently, the tandem N- and C-terminal SH2 domains of ZAP-70 (Hatada *et al.*, 1995) and the C-terminal SH2 from the closely related tyrosine kinase Syk (Narula *et al.*, 1995), in complex with a doubly tyrosine-phosphorylated peptide and a single phosphotyrosine pentapeptide, respectively. The core of the domain is formed by a central β-sheet flanked by two α-helices; loop regions of variable length, some containing additional segments of β-sheet, link these elements in the various structures. The prototypical SH2–target interactions were revealed in detail by crystal structures of high-affinity peptide complexes of the Src and Lck domains (Eck *et al.*, 1993; Waksman *et al.*, 1993). The binding mode of the peptide has been likened to a two-pin plug engaging in a two-hole socket, the larger 'hole' comprising the phosphotyrosine binding site and the smaller the recognition pocket for the pY+3 residue (isoleucine in both cases), on an otherwise rather flat surface. Numerous hydrogen bond and ion pair interactions between conserved SH2 residues and the phosphate oxygens and π ring electrons of the phosphotyrosine characterize the recognition at the pTyr site. The hydrophobic +3 pocket is formed by side chains of residues in the EF and BG loops and strand βD (in the terminology of Eck *et al.*). However, structures of peptide complexes of Syp (Lee *et al.*, 1994) and PLC-γ1 (Pascal *et al.*, 1994a) SH2 domains have revealed alternative recognition paradigms involving extended hydrophobic grooves for residues C-terminal to the pTyr.

The solution structure of the N-terminal SH2 domain from PI 3-kinase p85α was determined in the absence of bound peptide (Booker *et al.*, 1992). Subsequently, interactions of a 12 residue phosphopeptide encompassing the β-PDGF receptor pTyr751 site with this SH2 domain were probed by ^{1}H-^{15}N heteronuclear NMR (Hensmann *et al.*, 1994). These studies identified residues within the SH2 domain that are most closely involved in the binding interface, by monitoring backbone amide ^{1}H and ^{15}N chemical shifts and line widths upon titration of peptide into the SH2 sample. However, no detailed three-dimensional structural information has hitherto been available for phosphotyrosine peptide complexes of either PI 3-kinase SH2 domain. We present here the solution structure of a complex of the C-terminal SH2 domain of p85α (p85α-C SH2; ~38% sequence identity with the N-terminal domain) with a specific, high affinity tyrosine-phosphorylated pentapeptide. This peptide, acetyl-pTyr-Val-Pro-Met-Leu, is derived from the sequence of the pTyr751 binding site of the β-PDGF receptor. Many of the structural features of the complex revealed here, including the basis for the strong preference for methionine at pY+3, are likely to apply analogously to the N-terminal domain.

Results

A 112 residue domain (comprising residues 617–724 of human p85α plus four additional N-terminal residues derived from the thrombin cleavage site) was cleaved from the glutathione-*S*-transferase (GST) fusion protein and purified by cation exchange chromatography as described in Materials and methods. The freshly prepared, unliganded p85α-C SH2 domain gave well-dispersed NMR spectra, although long-term stability and solubility of the protein during extended data acquisition were poor unless the sample pH was maintained above 6.5 and the temperature below 25°C. Titration of the amino-terminally acetylated pTyr751 phosphotyrosine pentapeptide into a uniformly ^{15}N-labelled SH2 sample was monitored in a series of ^{1}H-^{15}N heteronuclear single-quantum correlation (HSQC) spectra. The majority of resonances were only slightly perturbed or, in some cases, completely unperturbed by this procedure. The intensity of amide resonances belonging to a number of residues closely involved in the binding interface diminished, and corresponding, shifted, bound-form resonances increased in intensity, as the peptide was titrated in. This process was not accompanied by any significant line broadening, indicating that the bound↔free exchange rate is within the slow exchange regime on the NMR chemical shift time scale. Indeed, the bound-form spectrum contained backbone amide resonances for some residues, later assigned to the BG loop region, which were absent (presumably due to extreme line broadening) from the free-form spectrum (*vide infra*). Full intensity of the bound-form spectrum and disappearance of corresponding free-form resonances was achieved at a 1:1 molar ratio of SH2 domain to peptide.

Resonance assignments for the uniformly ^{15}N,^{13}C-labelled SH2 domain and the unlabelled bound peptide were obtained from a combination of double- and triple-resonance three-dimensional (3D) and heteronuclear-filtered ^{1}H 2D experiments. ^{1}H-^{1}H nuclear Overhauser effect (NOE) correlations within the SH2 domain, within the peptide and between the SH2 domain and the peptide were then extracted from heteronuclear-filtered and -edited NOE datasets. Using these techniques, 68 NOE-derived distance restraints between the SH2 domain and the peptide, and 70 NOEs within the peptide, were included in the restraints list. The resulting total of 1326 interproton distance restraints was combined with 74 distance restraints for 37 hydrogen bonds and with 51 φ and χ dihedral angle restraints in dynamic simulated annealing (SA) structure calculations.

Description of the p85α-C SH2–peptide complex structure

Nineteen final structures were selected on the basis of best fit to the experimental data following simulated annealing refinement. Figure 1 shows a superposition of the structures, with the SH2 domain (backbone heavy atoms) in green and the pTyr751 peptide (all heavy atoms) coloured according to atom type. The average root-mean-square deviation (RMSD) from the mean coordinate positions for this family of structures is 0.39 ± 0.04 Å for the main chain (N, Cα, C′) atoms of residues 6–60, 69–70 and 78–107 of the SH2 domain and all residues (1–5) of the peptide; the corresponding figure for all heavy atoms over these regions is 0.81 ± 0.05 Å [residues not included in these RMSD calculations are predominantly disordered as judged from the NMR data, and comprise the N- and C-terminal regions (1–5 and 108–112) and, most notably, almost the entire βD′, βE, βF and FB regions (residues 61–77), the only significantly ordered residues within this span being Phe69 (βE4) and Ala70 (EF1) (*vide infra*)]. The peptide binding interface is also well defined, with an average coordinate RMSD from the

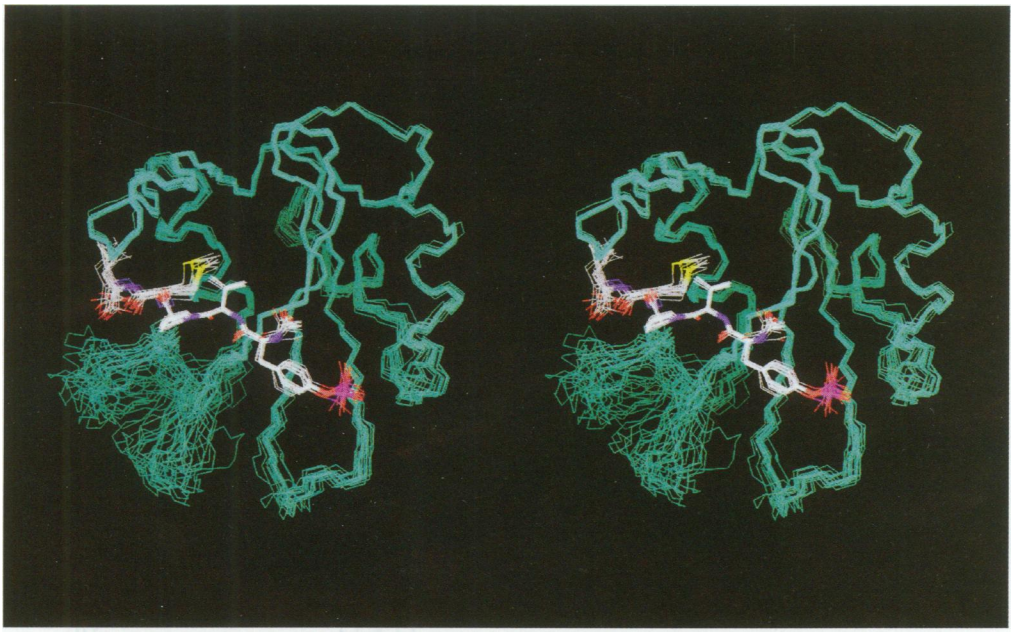

Fig. 1. Stereo view of a superposition of the 19 refined structures of the p85α-C SH2–β-PDGF receptor pTyr751 peptide complex. The backbone heavy atoms of the SH2 domain are shown in green, with all heavy atoms of the peptide shown coloured according to atom type. N- and C-terminal residues 1–5 and 108–112 of the SH2 domain are disordered and have been omitted for clarity in this and subsequent figures.

mean structure of 0.79 ± 0.08 Å for all heavy atoms of the SH2 and peptide residues comprising the interface. None of the final structures has distance restraint violations greater than 0.3 Å or torsion angle restraint violations greater than 3°, and the agreement with idealized covalent geometry is good; structural statistics are shown in Table I.

The core structure of helices αA and αB flanking the central β-sheet (comprising strands βA, βB, βC, βD and βG) is very similar to that of other SH2 domains whose structures have been determined. For example, when the core helical and sheet residues of the restrained, energy-minimized average structure of the p85α-C SH2 (12–14, 18–26, 33–37, 45–50, 55–60, 79–88 and 101–106) are superimposed on the corresponding positions of the Lck SH2 domain in its specific peptide complex (Eck *et al.*, 1993), the RMSD for Cα atoms is 0.83 Å (Figures 2 and 3). The bound peptide also adopts a very similar, extended backbone conformation to that found for other SH2 domains, lying roughly perpendicular to the central β sheet across the surface of the domain. However, the peptide backbone is drawn somewhat closer in towards the SH2 domain at the pY+3 and pY+4 positions in p85α-C than in Lck or Src.

Many of the differences between the ligand-bound or ligand-free SH2 domain structures determined to date are found in the connecting loop regions, which are of variable length (e.g. Figure 2) and which play a role in determining the specificity of binding and possibly in directing interactions with neighbouring domains or other proteins. However, some differences also arise from variability at positions within the structural core of the domain which display direct interactions with the bound peptide. The p85α-C SH2 complex is characterized by (i) a hydrophobic peptide binding channel created partly by the long BG loop, (ii) a phosphotyrosine binding pocket constructed from a comparatively short 'phosphate binding' (BC) loop, and (iii) disorder in solution in the βD′, βE, βF and FB regions. Schematic representations of the observed SH2–peptide intermolecular NOE and inferred hydrogen bond interactions are shown in Figure 4, while Figure 5 shows a heavy atom superposition of the peptide binding site of the 19 refined structures.

Interactions at the pTyr binding site

Compared with most SH2 domains of known sequence, the p85α-C SH2 has a short BC loop, being, for example, one residue shorter than that of Src, Lck, Syp-N or PLC-γ1-C domains and two shorter than in p85α-N SH2 (Figure 2). In consequence, the backbone of the domain adopts a slightly different conformation in this region from that in Src or Lck. In both the latter, a network of hydrogen bonds is formed involving the backbone amides of the BC1 and BC2 residues, the Ser or Thr BC2 side chain, and the phosphate oxygens of the peptide pTyr. In addition, the BC3 side chain (Thr) forms a bridging hydrogen bond to the terminal amino group of Lys βD6. The shorter p85α-C BC loop instead 'folds up' to bring the side chain of Ser βB7 within hydrogen bonding distance of the phosphate oxygens of the peptide pTyr (Figures 5 and 6A). The bridging hydrogen bond to the βD6 residue cannot be made since this position is occupied by a valine in p85α-C SH2; however, the lysyl side chain at BC2 in p85α-C SH2 is positioned such that its terminal amino group can make almost identical interactions with the pTyr to those made by Lys βD6 in other SH2s. This variation on the architecture of the pTyr binding site is likely to hold for other SH2 domains which have a Lys βD6 to Val mutation (e.g. vav, MUBPK), since they all also possess a lysine at position BC2. The hydrophobic side chains of Val βD6 and Ala βC3 form a platform for the phosphotyrosine ring, which is also constrained from the opposite side by interactions with the side chain methylene protons of His βD4 (Figures 5 and 6A).

In the Src– and Lck–peptide complex crystal structures,

Table I. Structural statistics for the 19 refined structures of p85α-C SH2–peptide complex

	<SA>	$(SA)_r$
RMS deviations from experimental distance restraints (Å)[a]		
All (1404)	0.033 ± 0.002	0.029
Interproton distances		
Intraresidue SH2 (324)	0.041 ± 0.002	0.039
Sequential SH2 (367)	0.034 ± 0.002	0.029
Short range SH2 ($1 < \|i–j\| \leq 4$) (184)	0.035 ± 0.004	0.031
Long range SH2 ($\|i–j\| > 4$) (313)	0.030 ± 0.003	0.021
Intrapeptide (70)	0.002 ± 0.002	0.0
Intermolecular SH2–peptide (68)	0.018 ± 0.003	0.018
H bonds (74)[b]	0.031 ± 0.005	0.020
RMS deviations from experimental dihedral restraints (°) (51)[a,c]	0.400 ± 0.090	0.396
Deviations from idealized covalent geometry		
Bonds (Å)	0.002 ± 0.0	0.002
Angles (°)	0.551 ± 0.008	0.533
Impropers (°)	0.356 ± 0.012	0.329
F_{NOE} (kJ/mol)[d]	197.3 ± 18.4	147.5
F_{CDIH} (kJ/mol)[e]	2.2 ± 1.1	2.0
F_{REPEL} (kJ/mol)[f]	55.2 ± 10.9	50.0
Cartesian coordinate RMS deviations (Å)	SH2 + peptide[g]	Binding interface only[h]
<SA> vs $(SA)_r$ (N, Cα, C′ atoms)	0.39 ± 0.04	–
<SA> vs $(SA)_r$ (all heavy atoms)	0.81 ± 0.05	0.79 ± 0.08

Statistics are listed for the 19 refined structures, <SA>, and for the restrained, energy-minimized mean structure, $(SA)_r$. The number of each type of restraint is indicated in brackets.
[a]None of the structures exhibit distance restraint violations >0.3 Å or dihedral violations >3°.
[b]Hydrogen bonds are characterized by two distance restraints each, $d_{N–O}$ = 2.7–3.3 Å and $d_{H–O}$ = 1.7–2.3 Å.
[c]Dihedral restraints comprise both backbone φ torsion angles and side chain χ torsion angles.
[d]NOE restraints were applied using a square-well potential with a force constant of 210 kJ/mol/Å^2.
[e]Torsion angle restraints were applied with a force constant of 840 kJ/mol/rad^2.
[f]The value of the quartic van der Waals repulsion term F_{REPEL} was calculated using a force constant of 17 kJ/mol/Å^4 and the hard sphere van der Waals radii set to 0.75 times their values in the parameter set parallhdg.pro.
[g]Excluding disordered residues 1–5, 61–68, 71–77 and 108–112.
[h]Comprises residues R19, R37, S39, K41, A46, V49, K56, H57, C58, V59, F69, A70, L91, H94, N95 and L98 of the SH2 domain and all residues of the peptide.

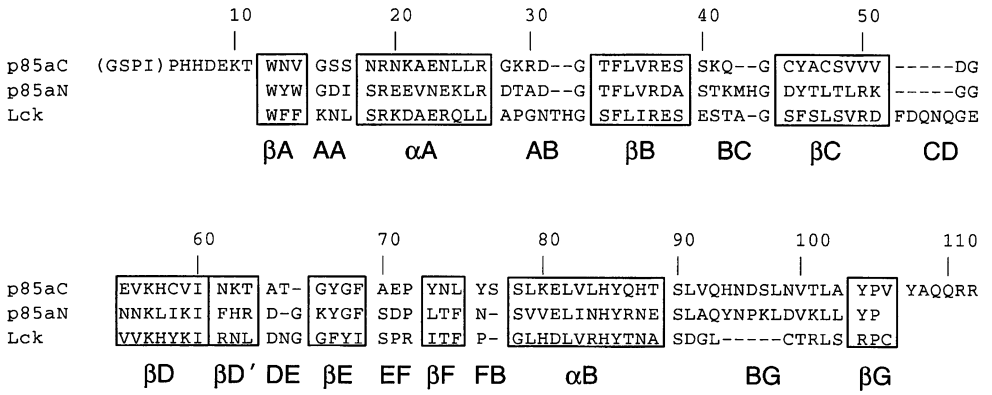

Fig. 2. Sequence of the p85α C-terminal SH2 domain construct aligned with the p85α N-terminal and Lck SH2 domain sequences. Secondary structure elements corresponding to those of Src SH2 are boxed and labelled using the nomenclature introduced by Eck *et al.* (1993). Residue numbers are those of the p85α-C SH2 protein used in the present study; bracketed residues at the N-terminus arise from the expression vector.

both arginines αA2 and βB5 form hydrogen bond interactions through their terminal guanidino groups to phosphate oxygens of the phosphotyrosine; the αA2 side chain also makes an 'amino-aromatic' interaction with the ring π-cloud (Waksman *et al.*, 1992, 1993; Eck *et al.*, 1993). In the p85α-C SH2–peptide complex there is strong indirect evidence for a stable hydrogen bond interaction in solution between the Arg βB5 terminal guanidino group and the pTyr phosphate group in the form of distinct observed chemical shifts for the four NηH and two ^{15}Nη

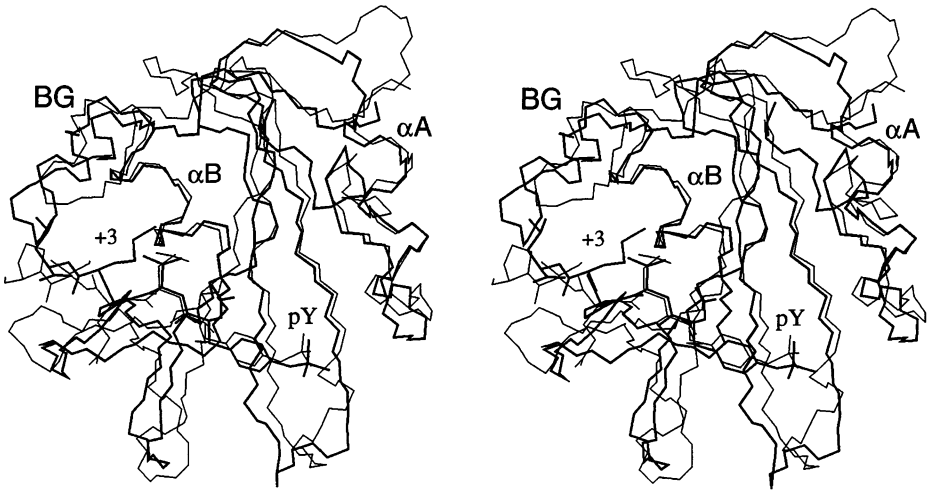

Fig. 3. Comparison of the p85α-C SH2– and Lck SH2–peptide complexes in stereoview. The restrained, energy-minimized average structure of the p85α-C SH2–peptide complex (heavy line) was superimposed on the Cα positions of the core secondary structure elements of the Lck–peptide complex (Eck *et al.*, 1993; light line). All heavy atoms of the peptide residues pTyr to pTyr+4 are shown, with the SH2 domains as backbone traces. The orientation is similar to that in Figure 1. The longer BG loop of the p85α-C SH2 and the displacement in position of the peptide +3 Met compared with the +3 Ile of the Lck complex can be seen.

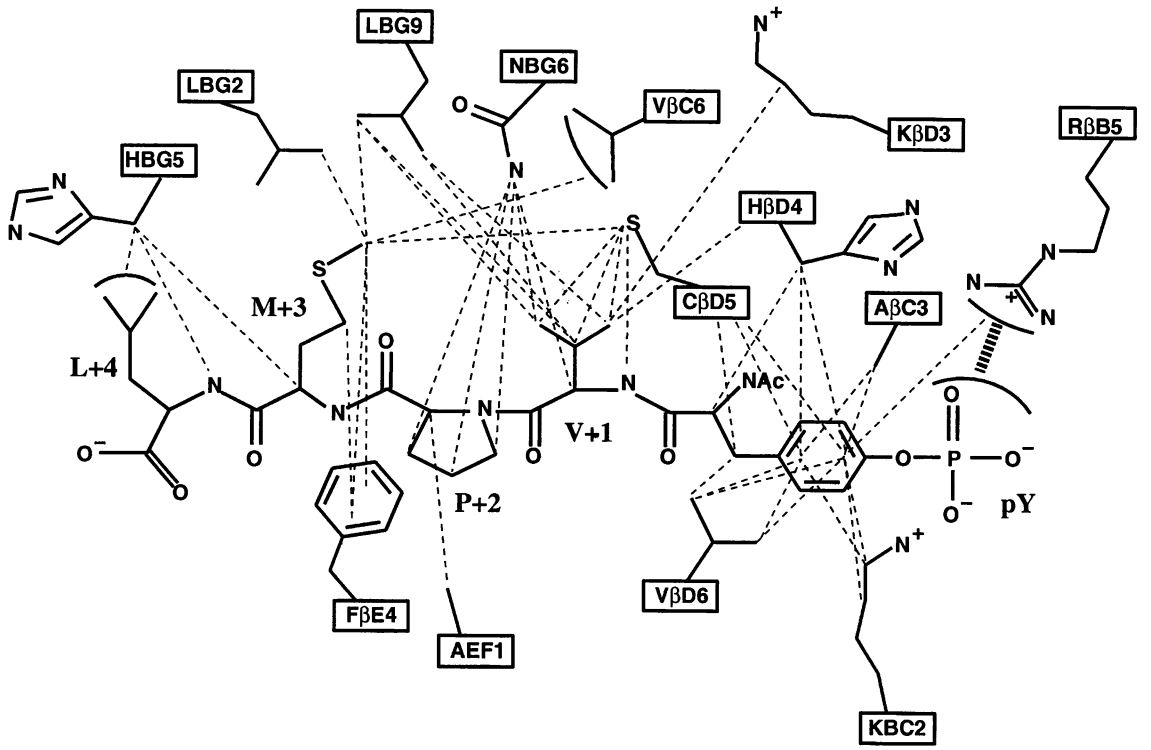

Fig. 4. Schematic depiction of the major NOE interactions observed between the SH2 domain and the peptide. NOEs, or clusters of NOEs arising from closely grouped protons, are shown as dashed lines emanating from the corresponding heavy atoms and indicate distances less than ~5 Å. Also shown (in heavy dashed line) is the inferred hydrogen bond interaction between RβB5 and the pTyr phosphate group. SH2 residues are labelled according to the convention of Eck *et al.* (1993).

resonances, with two of the NηH resonances being shifted substantially downfield of their random coil values. Distinct resonances for these nuclei are not normally observed at around neutral pH (6.8 in the present study) due to a combination of conformational averaging and fast exchange with solvent protons; the burial of Arg βB5 at the base of the pTyr binding pocket and the formation of stable hydrogen bonds presumably serve to slow these exchange processes sufficiently to allow their observation. In none of the NMR studies of SH2–phosphopeptide complexes published to date have any direct NOE interactions been observed between either conserved arginine side chain and the phosphotyrosine, presumably because the relevant distances between non-labile protons on the respective groups are too great and/or exchange broadening prevented observation of NOEs arising from the labile NεH or NηH protons. In contrast, in the present study, there is clear evidence from 2D F_1 ($^{15}N/^{13}C$)-filtered NOESY and unfiltered 3D CN-NOESY-HSQC spectra for direct NOEs between two of the four NηH proton

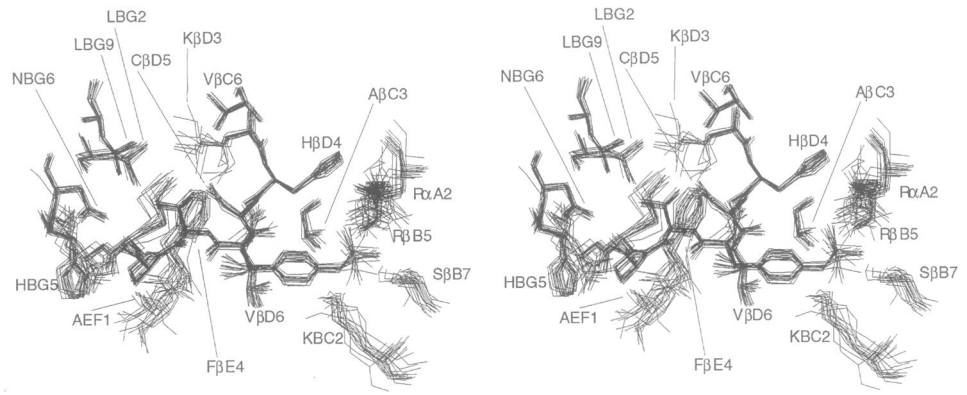

Fig. 5. All heavy-atom superposition of the binding interface between the SH2 domain and the peptide for the 19 refined structures, shown in stereoview. The orientation is approximately the same as in Figure 1. Residues of the SH2 domain involved in the binding interface are labelled according to the convention of Eck *et al.* (1993).

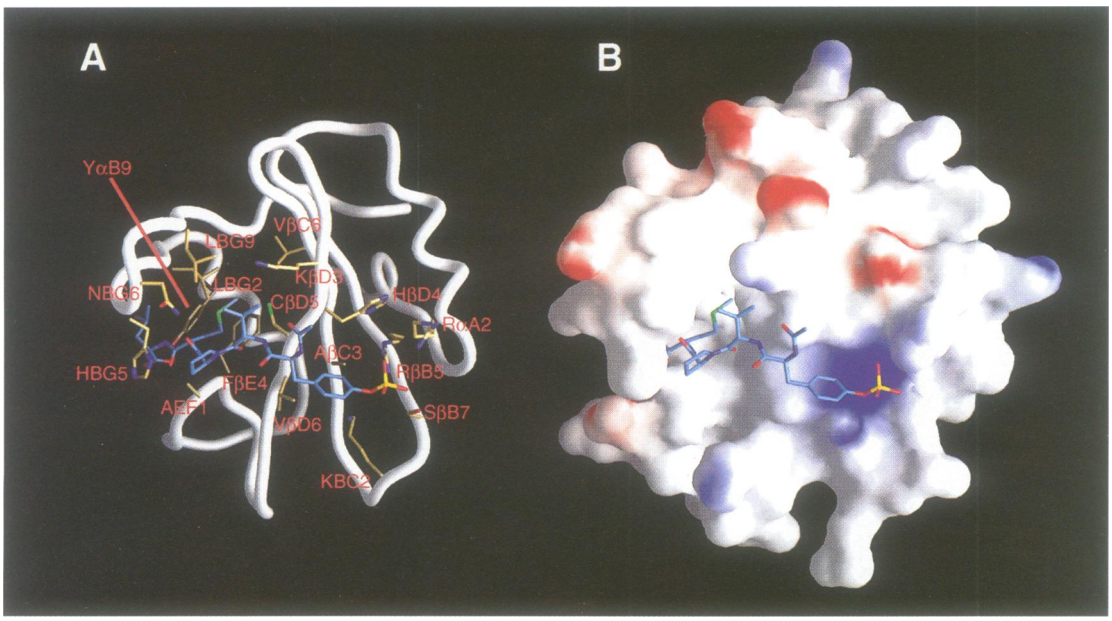

Fig. 6. (**A**) View of the restrained, minimized average structure of the p85α-C SH2–peptide complex. SH2 residues involved in the major binding interactions (labelled) are shown with gold carbon atoms, with the peptide having pale blue carbon atoms. The backbone (residues 6–107) of the SH2 domain is shown as a white tube. (**B**) Same view as in (A), but with the SH2 domain depicted as a molecular surface. Surface electrostatic potential is shown in red (negative) and blue (positive), with white representing neutral potential. The figure was generated using the program GRASP (Nicholls *et al.*, 1991; Nicholls, 1993).

resonances and the CεH ring protons of the pTyr (Figure 7). The side chain of Arg βB5 is also restrained by NOEs from NηH and NεH protons to the slowly exchanging hydroxyl proton of Ser βC5 (Figure 7); in the crystal structures of Src, Lck and Syp SH2–peptide complexes, the hydroxyl oxygen of this serine is hydrogen bonded to the Nε atom of Arg βB5.

In contrast to Arg βB5, distinct shifts are not observed for the NηH or ^{15}Nη resonances of Arg αA2, suggesting that interactions made by this side chain are somewhat more labile than those of Arg βB5; this might be a consequence of greater solvent accessibility. Despite this, the conformation of this side chain is partially defined by NOEs to the CδH and CεH ring protons of His βD4 and occupies a position up to its Cδ similar to that observed in crystal structures of the Src– and Lck–peptide complexes (Waksman *et al.*, 1992, 1993; Eck *et al.*, 1993).

Interactions C-terminal to the pTyr

Crystal structures of SH2–peptide complexes show the presence of a hydrogen bond between the backbone amide of the pTyr+1 residue of the peptide and the carbonyl oxygen of βD4 of the SH2 domain. The NH proton of +1 Val has a perturbed rate of exchange with solvent protons, as judged from the absence of a cross-peak at the water frequency in an F_1,F_2 (^{15}N/^{13}C)-filtered NOESY dataset acquired without saturation of the water resonance; since it is consistently within hydrogen bonding distance of, and in a favourable orientation to, the carbonyl oxygen of His βD4 in structures calculated without an explicit hydrogen bond restraint, it can be inferred that this interaction is also present in p85α-C SH2. The side chain of +1 Val lies in a shallow, apolar depression formed by the side chains of a number of residues of the SH2 domain including Lys βD3, Cys βD5 and Leu BG9, and makes

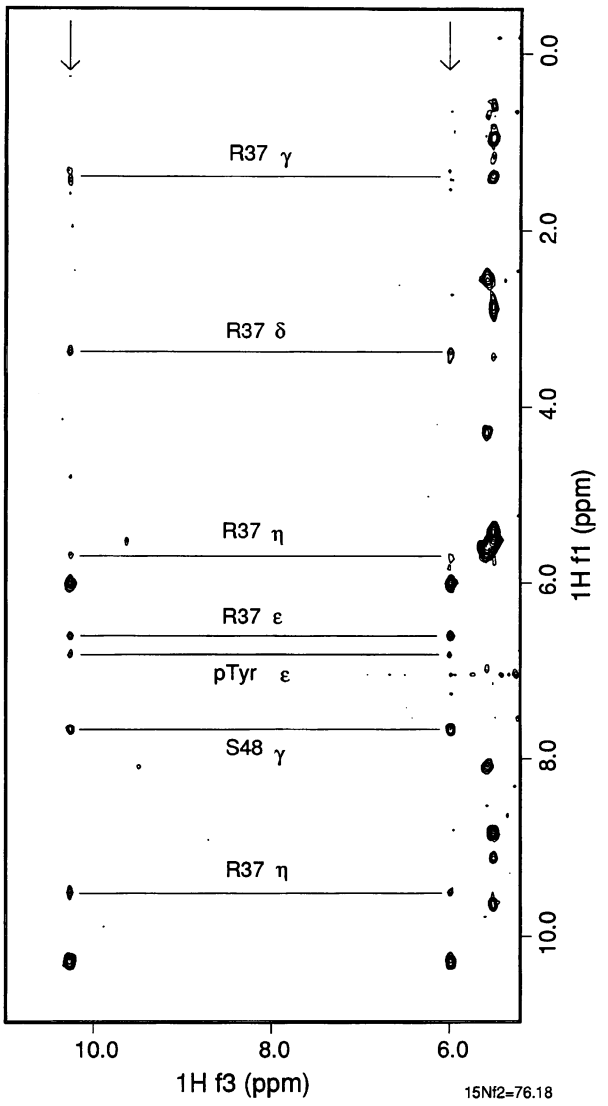

Fig. 7. Portion of an F_2 ($^{13}C/^{15}N$) plane taken from the CN-NOESY-HSQC spectrum of uniformly $^{15}N,^{13}C$-labelled p85α-C SH2 domain complexed with unlabelled phosphotyrosine pentapeptide, displaying NOE interactions made by two of the guanidino Nη protons of Arg βD5 (R37), highlighted at their ^1H (F_3) shifts by arrows.

NOE interactions with all of them and with Asn BG6 (Figures 4 and 5). The carbonyl oxygen of +1 Val is in a similar orientation to that observed in crystal structures of a number of SH2–peptide complexes, in which this oxygen forms a water-mediated hydrogen bond to the backbone amide of the βD6 SH2 residue. Comparatively slow amide proton exchange observed in the present study for Val βD6 suggests that this interaction may also occur in solution.

The side chain of the peptide +2 Pro residue is orientated approximately away from the SH2 domain; nevertheless, its position is well defined by NOEs to the side chain amide protons of Asn BG6. These protons display slow solvent exchange rates as judged from the absence of cross-peaks at the F_1 water frequency in the 3D CN-NOESY-HSQC experiment, and are within hydrogen bonding distance of the appropriately orientated carbonyl oxygen of +2 Pro (Figures 5 and 6A).

Interactions at the pTyr +3 'specificity' site

The backbone of the peptide beyond the C′ of +2 Pro is drawn in closer towards the SH2 domain than in (for example) the Lck or Src structures (Figure 3). This is also shown in the molecular surface representation (Figure 6B). The channel created by the BG and EF loops and the underlying side chains is almost entirely hydrophobic in nature. At the centre of this channel is a deeper pocket in which the side chain of the +3 methionine is buried. The walls of this +3 pocket are formed by the side chains of Phe βE4, Cys βD5, Leu BG9, Leu BG2 and Tyr αB9, while its base is formed by Cys βC4 and Val βC6. Restraining NOE interactions were observed between the terminal CεH methyl protons of +3 Met and side chain protons of Phe βE4, Cys βD5, Leu BG9 and Leu BG2. The degree of protection from solvent within this +3 binding pocket is evinced by the observation of numerous NOEs arising from the slowly exchanging thiol protons of both cysteines βC4 and βD5, including, in the latter case, interactions with the CεH methyl protons of +3 Met (Figures 4, 5 and 6A).

The bulky side chain of Phe βE4 results in a shift in the position of the +3 pocket compared with that seen in Src family SH2–peptide complexes (Figure 3), since it partially occludes the space that is occupied by the corresponding peptide side chain in these other structures. The +3 residue is no longer able to make interactions with the side chain of Tyr αB9 (Figure 6A), but rather is diverted back towards the central β-sheet, where the cysteine side chain of βD5 occupies less space than the corresponding tyrosine in Src, Lck, ZAP-70 and Syk-C. The location and narrowness of the +3 pocket resulting from these differences ensures that only the long, narrow and flexible hydrophobic side chain of methionine can make the optimal number of van der Waals contacts while avoiding unfavourable steric clashes.

Interactions beyond +3 Met

The leucine at +4 in the peptide makes less extensive contact with the SH2 domain than does the +3 residue. NOE contacts were observed between its Cδ methyl protons and the CβH protons of His BG5 (Figure 4). However, the conformation of +4 Leu is, in general, less well defined than that of the rest of the peptide. The lack of very extensive intermolecular interactions displayed by this residue is consistent with the low degree of sequence selectivity encountered at this position within phosphopeptide sequences predicted to be recognized by p85α SH2 domains (Songyang *et al.*, 1993); however, in the present case, the influence of truncation of the sequence after the +4 residue cannot be ruled out completely as a source of the greater disorder at this position.

Dynamic effects of peptide binding

A notable feature of NMR spectra of the unliganded p85α-C SH2 domain was the extreme broadening or complete absence of detectable resonances for the majority of residues in strands βD′, βE, βF and the FB loop (with the exception of Phe βE4 and Ala EF1), and for four residues (His BG5, Asn BG6, Asp BG7 and Ser BG8) in the BG loop (data not shown) under the experimental conditions used in this study. Effects of this nature are consistent with conformational exchange behaviour on a

microsecond to millisecond time scale. Structures of the unliganded domain (calculated with 1164 experimental restraints), while very similar overall to the peptide-complexed domain structure presented here, displayed very marked disorder in these regions, consistent with a lack of structurally significant NOEs (not shown). Addition of stoichiometric amounts of the specific phosphotyrosine pentapeptide resulted in the sharpening (or reappearance in the spectra) of all resonances of the BG5–BG8 residues, together with a number of NOE correlations arising from this stretch, both within the SH2 domain and between the SH2 and the bound peptide. However, the broadening in the βD′, βE, βF and FB regions persisted following binding of peptide.

Disorder at the distal end of the BG loop was also observed for the unliganded p85α N-terminal SH2 domain (Booker *et al.*, 1992; Hensmann *et al.*, 1994), but was not accompanied by significantly broadened lines in the absence of peptide. Nor was there line broadening in the βD′, βE, βF and FB regions of unliganded p85α-N SH2; indeed, this part of the molecule is well ordered in the calculated structures (Booker *et al.*, 1992). In contrast to the findings with p85α-C SH2 described here, however, titration of a 12 residue phosphotyrosine peptide derived from the sequence surrounding Tyr751 of the β-PDGF receptor into the p85α-N SH2 induced moderate to severe line broadening for a number of residues in the EF and BG loops, implying the presence of some form of microsecond to millisecond time scale exchange behaviour in the complex, but not in the free domain (Hensmann *et al.*, 1994).

Discussion

We have determined the structure of a high-affinity complex between the C-terminal SH2 domain of PI 3-kinase p85α and a specific phosphotyrosine pentapeptide derived from the Tyr751 binding site of the β-PDGF receptor using multinuclear, multidimensional NMR methods. Overall, the structure is well defined by the NMR data, with an average RMSD from the mean coordinates for the 19 refined structures of 0.39 ± 0.04 Å for the main chain (N, Cα, C′) atoms of the structurally restrained protein and peptide residues. The binding interface between peptide and SH2 domain is similarly well defined, with an average coordinate RMSD from the mean structure of 0.79 ± 0.08 Å for all heavy atoms of peptide and SH2 residues involved in binding. This level of definition has permitted the detailed structural analysis of many of the determinants of binding specificity displayed by this class of SH2 domain.

The most notable feature of the sequence specificity of the two SH2 domains of PI 3-kinase is their strong preference for methionine at the pY+3 position (Songyang *et al.*, 1993). This is manifested in the sequence contexts of Tyr740 (pYMDM) and Tyr751 (pYVPM) of the kinase insert of the β-PDGF receptor, both of which become phosphorylated following binding of PDGF to the extracellular portion of the receptor. Both these sequences display high affinity for the C-terminal SH2, although some data indicate that only the pTyr751 sequence binds tightly to the N-terminal SH2 (Klippel *et al.*, 1992; Panayotou *et al.*, 1993). Other known sites of association between PI 3-kinase p85α and signalling proteins include the colony-stimulating factor 1 receptor kinase insert, c-Kit, the insulin receptor substrate 1 protein, and polyomavirus middle-T antigen (Otsu *et al.*, 1991; Backer *et al.*, 1992; Lev *et al.*, 1992; Reedijk *et al.*, 1992), all of which contain the pY–hydrophobic–X–M motif.

The structure reported here gives some insights into the selectivity for methionine displayed by the p85 SH2 domains: the partial occlusion and displacement of the +3 binding site resulting from the intrusion of Phe βE4 leaves a pocket into which only methionine can fit optimally without unfavourable steric clashes. However, Met is not the only residue encountered at the pTyr+3 position in proteins known to associate with PI 3-kinase via its SH2 domains: the hepatocyte growth factor/scatter factor receptor binds through the sequence pYVXV, while Flt-1 tyrosine kinase receptor is reported to contain a pYVNA recognition sequence for PI 3-kinase (Ponzetto *et al.*, 1993; Cunningham *et al.*, 1995). In the former case, it was demonstrated that the affinity of the p85 N- and C-terminal SH2 domains for the pYVXV site is some two orders of magnitude weaker than the corresponding interaction with the β-PDGF receptor pTyr751 sequence (Ponzetto *et al.*, 1993). It seems possible that the effect of a non-optimal pTyr+3 residue may be compensated in some cases by a bidentate interaction between both p85 SH2 domains and optimally spaced pTyr binding sites, either on the same receptor chain or on neighbouring chains of an activated receptor dimer (Ponzetto *et al.*, 1993; Cunningham *et al.*, 1995).

Interaction of the p85 subunit of PI 3-kinase with the p110 catalytic subunit has been shown to occur through the 'inter-SH2' region of ~160 residues which lies between the N- and C-terminal SH2 domains (Klippel *et al.*, 1993). It is interesting to speculate, in the light of the recent X-ray crystal structure of the tandem ZAP-70 N- and C-SH2 domains complexed with a doubly tyrosine-phosphorylated peptide from the T-cell receptor ζ-chain (Hatada *et al.*, 1995), upon whether similarities might exist in overall architecture between ZAP-70 and p85. The ZAP-70 structure contains an α-helical coiled-coil inter-SH2 domain of ~60 residues which folds in such a manner as to bring the N- and C-terminal SH2 domains into very close apposition, to the extent that the N-SH2 has an 'incomplete' phosphotyrosine binding site which is completed by side chains from the neighbouring C-SH2. The paired domains bind the peptide, whose twin phosphotyrosine residues are 11 positions apart, in a 'head-to-tail' formation. Neither individual expressed ZAP-70 SH2 domain binds the ζ-chain peptide or other sequences with high affinity, suggesting that the close association of the two SH2 domains is functionally essential. Although, unlike ZAP-70, both p85α SH2 domains are individually capable of binding to specific tyrosine-phosphorylated sequences with high affinity, it is conceivable that the N- and C-terminal SH2 domains of p85 are brought similarly close together within the intact protein. This would be geometrically consistent with the suggestion that p85 binding to the activated β-PDGF receptor may be mediated by binding of the C-terminal SH2 domain to the pTyr740 site and the N-terminal domain to the pTyr751 site (Panayotou *et al.*, 1993). Here, we have observed conformational exchange behaviour (as judged by extreme

line broadening) for the p85α-C SH2 in the βD′, βE, βF and FB regions, a part of the domain that has a well-defined β-sheet structure in all other solved SH2 domains. Presence of interdomain contacts in the intact p85, but not in the excised SH2, might account for these observations.

Materials and methods

Expression and purification of p85α C-terminal SH2 domain

The gene sequence of the C-terminal SH2 domain of human p85α, comprising residues 617–724 of the full-length protein (Skolnik *et al.*, 1991), was amplified by polymerase chain reaction and subcloned initially into the pGEX3X (Pharmacia) expression vector. For expression of GST fusion protein destined for NMR studies, the domain sequence was subcloned into the vector pGEX2T (Pharmacia). The resultant plasmid, pZen1532, was transformed into a derivative ($lacI^Q$) of *Escherichia coli* W3110 (CGSC 6564: E.Coli Genetic Stock Center, Yale). GST fusion protein uniformly enriched (>98%) with ^{15}N and ^{13}C was prepared by growing *E.coli* cells in M9-ampicillin minimal medium containing 0.3 g/l [^{15}N]ammonium sulfate and 0.625 g/l [^{13}C]glucose (final) after inoculation from a pre-culture grown in M9-ampicillin minimal medium containing 1 g/l [^{15}N]ammonium sulfate and 2 g/l [^{13}C]glucose and supplemented with 0.02% (w/v) casein hydrolysate. When the cell density reached OD_{550} = 0.2–0.3, GST–p85α-C SH2 fusion protein expression and accumulation was induced by adding IPTG (isopropyl β-D-thiogalactopyranoside) to a final concentration of 0.1 mM. After 5 h, bacteria accumulating soluble fusion protein at ~20% of the total cell protein were harvested and resuspended in 20 mM Tris–HCl pH 7.4, 150 mM NaCl, 1 mM EDTA and 0.1 mg/ml lysozyme (Sigma). Following lysis, the supernatant was bound to glutathione–Sepharose 4B (Pharmacia), and GST–p85α-C SH2 fusion protein was affinity purified by elution with 50 mM Tris–HCl (pH 8.0), 20 mM NaCl and 10 mM reduced glutathione (Sigma).

The fusion protein was cleaved using thrombin (Sigma) and loaded directly onto a Mono-S cation-exchange column (Pharmacia) pre-equilibrated in 20 mM sodium phosphate (pH 7.4) and 20 mM dithiothreitol (DTT). The protein was eluted using a NaCl gradient (0–0.15 M) in the same buffer. A single peak containing p85α-C SH2 was eluted at ~0.06 M NaCl. Purity was >95% as estimated by SDS–PAGE, and the N-terminus was confirmed by Edman sequencing. Both electrospray–ionization mass spectrometry and matrix-assisted laser desorption time-of-flight mass spectrometry gave the expected molecular mass.

Peptide synthesis

The pentapeptide Ac-pTyr-Val-Pro-Met-Leu-OH, corresponding to the sequence surrounding Tyr751 of the β-PDGF receptor, was synthesized by the solid-phase Fmoc strategy, coupling with 2-(1H-benzotriazol-1-yl)-1,1,3,3-tetramethyluronium hexafluorophosphate (HBTU) and incorporating Fmoc-phosphotyrosine without protection of the phosphate group. After acetylation, the peptide was cleaved from the resin with trifluoroacetic acid and purified by preparative reverse-phase (RP) HPLC. The peptide was characterized by mass spectrometry, amino acid analysis and both RP and anion-exchange HPLC (>95% purity).

NMR spectroscopy

Protein samples for NMR spectroscopy were prepared in argon-purged buffers containing 50 mM sodium phosphate, 50 mM NaCl, 2.0 mM DTT-d_{10}, 0.1 mM EDTA, 0.01% (w/v) NaN_3 and 8% D_2O at pH 6.8. Buffer exchange and concentration were effected over 10 kDa cutoff ultrafiltration membranes; final protein concentrations were 1.0–1.2 mM in sample volumes of 0.55 ml. Stoichiometric complexes of peptide with SH2 domain were routinely prepared in the following way. Approximately 1.5 molar equivalents of peptide were added from a concentrated stock in buffer to an SH2 NMR sample; the complex was then subjected to 2–3 cycles of 5-fold dilution with sample buffer and reconcentration as above. Samples were blanketed with argon after transfer into NMR tubes.

NMR experiments were carried out at a sample temperature of 23°C on a three-channel Varian Unity 600 MHz instrument equipped with waveform generators and a pulsed-field gradient module. All triple-resonance experiments and most of the heteronuclear-filtered experiments were adapted to incorporate *z*-gradient pulses to aid in suppression of artifacts and for elimination of the water resonance. Gradients were not, in general, used for coherence selection. For most heteronuclear experiments involving detection of NH protons, pulsed-field gradients were combined with the use of water-selective RF pulses to place the water magnetization along the *z*-axis during most of the pulse sequence and acquisition (Grzesiek and Bax, 1993a; Kay *et al.*, 1994; Stonehouse *et al.*, 1994); this was particularly useful in maximizing sensitivity for all resonances in the present case due to the high sample pH and consequently high intrinsic rate of amide proton exchange. Sequential assignment and collection of intraprotein NOEs were achieved for the SH2 domain using the following 3D gradient experiments: triple-resonance CBCA(CO)NH (Grzesiek and Bax, 1992), HBHA(CBCA-CO)NH (Grzesiek and Bax, 1993b) and HNCACB (Wittekind and Müller, 1993), ^{15}N-separated TOCSY-HSQC (Marion *et al.*, 1989), ^{15}N-separated NOESY-HSQC (Marion *et al.*, 1989) (120 ms mixing time), ^{13}C-separated HCCH-TOCSY (Kay *et al.*, 1993) and simultaneous ^{15}N/^{13}C-separated CN-NOESY-HSQC (Pascal *et al.*, 1994b) (120 ms mixing time). The ^{13}C-separated HCCH-TOCSY experiment was modified to incorporate a 'semi-constant time' ^1H (t_1) evolution period (Grzesiek and Bax, 1993) to improve resolution in this dimension. In addition to the 3D heteronuclear datasets, various homonuclear ^1H 2D datasets were also acquired, including a 120 ms mixing time NOESY dataset recorded at 750 MHz on the in-house-built instrument of the Oxford Centre for Molecular Sciences (OCMS). Three-bond NH-CαH coupling constants were measured by line-shape fitting F_1 traces from a HMQC-J dataset (Kay and Bax, 1990). Qualitative estimates of amide proton exchange rates were obtained from examination of cross-peak intensities in an F_1 slice of the 3D CN-NOESY-HSQC dataset (acquired using pulsed-field gradients and without solvent pre-saturation) taken at the chemical shift of the water resonance.

For assignment of resonances of the unlabelled bound peptide and for recording of intrapeptide NOE interactions, doubly isotope-filtered 2D experiments were used, including F_1,F_2 (^{15}N/^{13}C)-filtered DQF-COSY, TOCSY and NOESY (Ikura and Bax, 1992; Petros *et al.*, 1992; Xu *et al.*, 1994). These experiments were all recorded in H_2O solution and employed pulsed-field gradient dephasing both in the heteronuclear filters and for water suppression using the WATERGATE technique (Piotto *et al.*, 1992). Intermolecular NOEs between the SH2 domain and the bound peptide were extracted from the following H_2O solution datasets: 2D F_1 (^{15}N/^{13}C)-filtered, F_2 (^{15}N/^{13}C)-edited NOESY (100 ms mixing time); 3D F_1 (^{15}N/^{13}C)-filtered simultaneous ^{15}N/^{13}C-separated CN-NOESY-HSQC (120 ms mixing time); and unfiltered 3D CN-NOESY-HSQC (120 ms mixing time).

NMR data were processed using FELIX version 2.3 (Biosym). Time-domain digital solvent filters and data extension by linear prediction were used where necessary. The NMRView software package (Johnson and Blevins, 1994) was used for spectral analysis.

Structure calculations

Three-dimensional structures were calculated from the restraint data using the program X-PLOR version 3.1 (Brünger, 1992; Molecular Simulations, Inc.) on an IBM RS/6000 Model 590 computer. Ensembles of structures with correct three-dimensional folds were generated from starting configurations having randomized backbone torsion angles using an *ab initio* dynamic simulated annealing (SA) protocol (Nilges *et al.*, 1988; Brünger, 1992), and were then subjected to further cycles of SA refinement (Nilges *et al.*, 1991; Downing *et al.*, 1992; Hommel *et al.*, 1992) with incorporation of additional restraints. The final values of the hard sphere van der Waals radii used by the REPEl function were set to 0.75 times their values in the parameter set parallhdg.pro (Brünger, 1992). Experimental NOE intensities were incorporated as distance ranges, with centre averaging and appropriate corrections for distances involving methyl, ring and non-stereospecifically assigned methylene protons. Stereospecific assignments for a number of methylene and γ- and δ-methyl proton resonances of the SH2 domain and the peptide were made based upon a combination of criteria, including (i) intraresidue and sequential NOE intensities, (ii) relative coupling constant values determined from ^1H-homonuclear- or heteronuclear-edited TOCSY experiments and (iii) examination of ensembles of structures in which the local environment of the side chain was already well defined and one distinct side chain orientation was displayed in a majority of structures. In the case of methylene protons, this analysis also yielded a dihedral angle restraint to the corresponding staggered side chain rotamer (±30°). Intra- and interresidue NOE intensities and relative coupling constant magnitudes from isotope-filtered datasets established both the χ^1 and χ^2 rotamer states as –60 ± 30° for the +3 Met side chain of the peptide and permitted stereospecific assignment of the Cβ and Cγ methylene proton pairs. Three-bond NH-CαH coupling constant data from the HMQC-J experiment were converted to dihedral angle ranges for the φ torsion angle as follows: for J<4.5 Hz for residues in regions

of known helical backbone conformation, ϕ was restrained to $-60 \pm 30°$; for $J>8$ Hz, ϕ was restrained to $130 \pm 30°$. Seventy four distance restraints were incorporated for 37 hydrogen bonds on the basis of qualitative assessment of NH exchange rates and after identification of the acceptors from structures calculated in the absence of hydrogen bond restraints. On the basis of the observation of distinct ^1H and ^{15}N chemical shifts for the (normally fast-exchanging) η guanidino resonances of Arg37 (βB5), a hydrogen bond distance restraint was incorporated between each Hη and a pseudoatom representing the phosphate oxygens positioned at the phosphorus atom.

Final structure calculations incorporated 1451 restraints, comprising 324 intraresidue, 367 sequential, 184 short-range ($1 < |i-j| \leq 4$) and 313 long-range ($|i-j| > 4$) NOE distance restraints for the SH2 domain, 70 intramolecular NOE restraints for the peptide, 68 intermolecular NOE restraints between the peptide and the SH2 domain, 74 hydrogen bond distance restraints and 51 torsion angle restraints.

The atomic coordinates of the 19 refined SA structures and the restrained, energy-minimized mean structure will be deposited with the Brookhaven Protein Data Bank.

Acknowledgements

The authors thank J.Boyd and N.Soffe (OCMS) for expert advice and assistance during acquisition of the 750 MHz data. The Oxford Centre for Molecular Sciences is thanked for access to the 750 MHz spectrometer.

References

Backer,J.M., Myers,M.G.,Jr, Shoelson,S.E., Chin,D.J., Sun,X.J., Margolis,B., Skolnik,E.Y., Schlessinger,J. and White,M.F. (1992) Phosphatidylinositol-3′-kinase is activated by association with IRS-1 during insulin stimulation. *EMBO J.*, **11**, 3469–3479.

Booker,G.W., Breeze,A.L., Downing,A.K., Panayotou,G., Gout,I., Waterfield,M.D. and Campbell,I.D. (1992) Structure of an SH2 domain of the p85α subunit of phosphatidylinositol-3-OH kinase. *Nature*, **358**, 684–687.

Brünger,A.T. (1992) *X-PLOR Version 3.1: A System for X-ray Crystallography and NMR*. Yale University Press, New Haven and London.

Cunningham,S.A., Waxham,M.N., Arrate,P.M. and Brock,T.A. (1995) Interaction of the Flt-1 tyrosine kinase receptor with the p85 subunit of phosphatidylinositol 3-kinase. *J. Biol. Chem.*, **270**, 20254–20257.

Downing,A.K., Driscoll,P.C., Harvey,T.S., Dudgeon,T.J., Smith,B.O., Baron,M. and Campbell,I.D. (1992) Solution structure of the fibrin binding finger domain of tissue-type plasminogen activator determined by ^1H nuclear magnetic resonance. *J. Mol. Biol.*, **225**, 821–833.

Eck,M.J., Shoelson,S.E. and Harrison,S.C. (1993) Recognition of a high-affinity phosphotyrosyl peptide by the Src homology-2 domain of p56^{lck}. *Nature*, **362**, 87–91.

Escobedo,J.A., Kaplan,D.R., Kavanaugh,W.M., Turck,C.W. and Williams,L.T. (1991) A phosphatidylinositol 3-kinase binds to platelet-derived growth factor receptors through a specific receptor sequence containing phosphotyrosine. *Mol. Cell. Biol.*, **11**, 1125–1132.

Fantl,W.J., Escobedo,J.A., Martin,G.A., Turck,C.W., del Rosario,M., McCormick,F. and Williams,L.T. (1992) Distinct phosphotyrosines on a growth factor receptor bind to specific molecules that mediate different signalling pathways. *Cell*, **69**, 413–423.

Grzesiek,S. and Bax,A. (1992) Correlating backbone amide and side chain resonances in larger proteins by multiple relayed triple resonance NMR. *J. Am. Chem. Soc.*, **114**, 6291–6293.

Grzesiek,S. and Bax,A. (1993a) The importance of not saturating H_2O in protein NMR. Application to sensitivity enhancement and NOE measurements. *J. Am Chem. Soc.*, **115**, 12593–12594.

Grzesiek,S. and Bax,A. (1993b) Amino acid type determination in the sequential assignment procedure of $^{13}C/^{15}N$-enriched proteins. *J. Biomol. NMR*, **3**, 185–204.

Hatada,M.H. *et al.* (1995) Molecular basis for interaction of the protein tyrosine kinase ZAP-70 with the T-cell receptor. *Nature*, **377**, 32–38.

Hensmann,M., Booker,G.W., Panayotou,G., Boyd,J., Linacre,J., Waterfield,M.D. and Campbell,I.D. (1994) Phosphopeptide binding to the N-terminal SH2 domain of the p85α subunit of PI 3′-kinase: a heteronuclear NMR study. *Protein Sci.*, **3**, 1020–1030.

Hiles,I.D., Otsu,M., Volinia,S., Fry,M.J., Gout,I., Dhand,R., Panayotou,G., Ruiz-Larrea,F., Thompson,A., Totty,N.F., Hsuan,J.J., Courtneidge,S.A., Parker,P.J. and Waterfield,M.D. (1992) Phosphatidylinositol 3-kinase: structure and expression of the 110 kDa catalytic subunit. *Cell*, **70**, 419–429.

Hommel,U., Harvey,T.S., Driscoll,P.C. and Campbell,I.D. (1992) Human epidermal growth factor: high resolution solution structure and comparison with human transforming growth factor α. *J. Mol. Biol.*, **227**, 271–282.

Ikura,M. and Bax,A. (1992) Isotope-filtered 2D NMR of a protein–peptide complex: study of a skeletal muscle myosin light chain kinase fragment bound to calmodulin. *J. Am. Chem. Soc.*, **114**, 2433–2440.

Johnson,B.A. and Blevins,R.A. (1994) NMRView: a computer program for the visualization and analysis of NMR data. *J. Biomol. NMR*, **4**, 603–614.

Kapeller,R. and Cantley,L.C. (1994) Phosphatidylinositol 3-kinase. *BioEssays*, **16**, 565–576.

Kashishian,A., Kazlauskas,K. and Cooper,J.A. (1992) Phosphorylation sites in the PDGF receptor with different specificities for binding GAP and PI 3-kinase *in vivo*. *EMBO J.*, **11**, 1373–1382.

Kay,L.E. and Bax,A. (1990) New methods for the measurement of NH-CαH coupling constants in ^{15}N-labelled proteins. *J. Magn. Reson.*, **86**, 110–126.

Kay,L.E., Xu,G.-Y., Singer,A.U., Muhandiram,D.R. and Forman-Kay,J.D. (1993) A gradient enhanced HCCH-TOCSY experiment for recording side-chain ^1H and ^{13}C correlations in H_2O samples of proteins. *J. Magn. Reson. (B)*, **101**, 333–337.

Kay,L.E., Xu,G.-Y. and Yamazaki,T. (1994) Enhanced-sensitivity triple-resonance spectroscopy with minimal H_2O saturation. *J. Magn. Reson. (A)*, **109**, 129–133.

Klippel,A., Escobedo,J.A., Fantl,W.J. and Williams,L.T. (1992) The C-terminal SH2 domain of p85 accounts for the high affinity and specificity of the binding of phosphatidylinositol 3-kinase to phosphorylated platelet-derived growth factor β receptor. *Mol. Cell. Biol.*, **12**, 1451–1459.

Klippel,A., Escobedo,J.A., Hu,Q. and Williams,L.T. (1993) A region of the 85-kilodalton (kDa) subunit of phosphatidylinositol 3-kinase binds the 110-kDa catalytic subunit *in vivo*. *Mol. Cell. Biol.*, **13**, 5560–5566.

Lee,C.-H., Kominos,D., Jacques,S., Margolis,B., Schlessinger,J. Shoelson,S.E. and Kuriyan,J. (1994) Crystal structures of peptide complexes of the amino-terminal SH2 domain of the Syp tyrosine phosphatase. *Structure*, **2**, 423–438.

Lev,S., Givol,D. and Yarden,Y. (1992) Interkinase domain of kit contains the binding site for phosphatidylinositol 3′ kinase. *Proc. Natl Acad. Sci. USA*, **89**, 678–682.

Marion,D., Driscoll,P.C., Kay,L.E., Wingfield,P.T., Bax,A., Gronenborn, A.M. and Clore,G.M. (1989) Overcoming the overlap problem in the assignment of ^1H NMR spectra of larger proteins by use of three-dimensional heteronuclear ^1H-^{15}N Hartmann–Hahn-multiple quantum coherence and nuclear Overhauser-multiple quantum coherence spectroscopy: application to interleukin 1β. *Biochemistry*, **28**, 6150–6156.

Narula,S.S. *et al.* (1995) Solution structure of the C-terminal SH2 domain of the human tyrosine kinase Syk complexed with a phosphotyrosine pentapeptide. *Structure*, **3**, 1061–1073.

Nicholls,A.J. (1993) *GRASP Manual*. Columbia University, New York.

Nicholls,A., Sharp,K.A. and Honig,B. (1991) Protein folding and association: insights from the interfacial and thermodynamic properties of hydrocarbons. *Proteins*, **11**, 281–296.

Nilges,M., Clore,G.M. and Gronenborn,A.M. (1988) Determination of three-dimensional structures of proteins from interproton distance data by hybrid distance geometry-dynamical simulated annealing calculations. *FEBS Lett.*, **229**, 317–324.

Nilges,M., Kuszewski,J. and Brünger,A.T. (1991) Sampling properties of simulated annealing and distance geometry. In Hoch,J.C., Poulsen,F.M. and Redfield,C. (eds), *Computational Aspects of the Study of Biological Macromolecules*. Plenum Press, New York, pp. 451–455.

Otsu,M. *et al.* (1991) Characterization of two 85 kDa proteins that associate with receptor tyrosine kinases, middle-T/pp60$^{c\text{-}src}$ complexes, and PI3-kinase. *Cell*, **65**, 91–104.

Overduin,M., Rios,C.B., Mayer,B.J., Baltimore,D. and Cowburn,D. (1992) Three-dimensional solution structure of the Src homology 2 domain of c-*abl*. *Cell*, **70**, 697–704.

Panayotou,G. *et al.* (1993) Interactions between SH2 domains and tyrosine-phosphorylated platelet-derived growth factor β-receptor sequences: analysis of kinetic pararmeters by a novel biosensor-based approach. *Mol. Cell. Biol.*, **13**, 3567–3576.

Pascal,S.M., Singer,A.U., Gish,G., Yamazaki,T., Shoelson,S.E., Pawson,T., Kay,L.E. and Forman-Kay,J.D. (1994a) Nuclear magnetic

resonance structure of an SH2 domain of phospholipase C-γ1 complexed with a high affinity binding peptide. *Cell*, **77**, 461–472.
Pascal,S.M., Muhandiram,D.R., Yamazaki,T., Forman-Kay,J.D. and Kay,L.E. (1994b) Simultaneous acquisition of ^{15}N and ^{13}C edited NOE spectra of proteins dissolved in H_2O. *J. Magn. Reson. (B)*, **101**, 197–201.
Pawson,T. and Schlessinger,J. (1993) SH2 and SH3 domains. *Curr. Biol.*, **3**, 434–442.
Petros,A.M., Kawai,M., Luly,J.R. and Fesik,S.W. (1992) Conformation of two non-immunosuppressive FK506 analogs when bound to FKBP by isotope-filtered NMR. *FEBS Lett.*, **308**, 309–314.
Piccione,E., Case,R.D., Domchek,S.M., Hu,P., Chaudhuri,M., Backer, J.M., Schlessinger,J. and Shoelson,S.E. (1993) Phosphatidylinositol 3-kinase p85 SH2 domain specificity defined by direct phophopeptide/SH2 domain binding. *Biochemistry*, **32**, 3197–3202.
Piotto,M., Saudek,V. and Sklenár,V. (1992) Gradient-tailored excitation for single-quantum NMR spectroscopy of aqueous solutions. *J. Biomol. NMR*, **2**, 661–665.
Ponzetto,C., Bardelli,A., Maina,F., Longati,P., Panayotou,G., Dhand,R., Waterfield,M.D. and Comoglio,P.M. (1993) A novel recognition motif for phosphatidylinositol 3-kinase binding mediates its association with the hepatocyte growth factor/scatter factor receptor. *Mol. Cell. Biol.*, **13**, 4600–4608.
Reedijk,M., Liu,X., van der Greer,P., Letwin,K., Waterfield,M.D., Hunter,T. and Pawson,T. (1992) Tyr721 regulates specific binding of the CSF-1 receptor kinase insert to PI 3′-kinase SH2 domains: a model for SH2-mediated receptor–target interactions. *EMBO J.*, **11**, 1365–1372.
Skolnik,E.Y., Margolis,B., Mohammadi,M., Lowenstein,E., Fischer,R., Drepps,A., Ullrich,A. and Schlessinger,J. (1991) Cloning of PI 3-kinase-associated p85 utilizing a novel method for expression/cloning of target proteins for receptor tyrosine kinases. *Cell*, **65**, 83–90.
Songyang,Z. *et al.* (1993) SH2 domains recognize specific phosphopeptide sequences. *Cell*, **72**, 767–778.
Stonehouse,J., Shaw,G.L., Keeler,J. and Laue,E.D. (1994) Minimizing sensitivity losses in gradient-selected ^{15}N-^{1}H HSQC spectra of proteins. *J. Magn. Reson. (A)*, **107**, 178–184.
Waksman,G. *et al.* (1992) Crystal structure of the phosphotyrosine recognition domain SH2 of v-*src* complexed with tyrosine-phosphorylated peptides. *Nature*, **358**, 646–653.
Waksman,G., Shoelson,S.E., Pant,N., Cowburn,D. and Kuriyan,J. (1993) Binding of a high affinity phosphotyrosyl peptide to the Src SH2 domain: crystal structures of the complexed and peptide-free forms. *Cell*, **72**, 779–790.
Wittekind,M. and Müller,L. (1993) HNCACB: a high sensitivity 3D NMR experiment to correlate amide proton and nitrogen resonances with the alpha- and beta-carbon resonances in proteins. *J. Magn. Reson. (B)*, **101**, 201–205.
Xu,R.X., Gampe,R.T.,Jr and Davis,D.G. (1994) Double-tuned isotope-filtered DQF-COSY. *J. Magn. Reson. (B)*, **105**, 180–182.
Xu,R.X., Word,J.M., Davis,D.G., Rink,M.J., Willard,D.H.,Jr and Gampe,R.T.,Jr (1995) Solution structure of the human pp60$^{c\text{-}src}$ SH2 domain complexed with a phosphorylated tyrosine pentapeptide. *Biochemistry*, **34**, 2107–2121.

Received on February 29, 1996; revised on March 27, 1996

Note added in proof

Crystal structures of the p85α N-terminal SH2 domain complexed with pTyr-hydrophobic-X-Met peptides were reported recently by S.C.Harrison and co-workers [Nolte,R.T. *et al.* (1996) *Nature Struct. Biol.*, **3**, 364–374]. The specificity-determining interactions made by the +3 Met peptide residue in these structures are similar to those reported here for p85α-C SH2.